Current-dependent potential for nonlocal absorption in quantum hydrodynamic theory

Cristian Ciracì[*]

Center for Biomolecular Nanotechnologies (CBN), Istituto Italiano di Tecnologia (IIT), Via Barsanti 14, 73010 Arnesano (LE), Italy

(Received 18 July 2016; revised manuscript received 6 June 2017; published 30 June 2017)

The quantum hydrodynamic theory is a promising method for describing microscopic details of macroscopic systems. The hydrodynamic equation can be partially obtained from a single-particle Kohn-Sham equation and improved by adding a viscoelastic kinetic-exchange-correlation tensor term, so that broadening of collective excitation can be taken into account, as well as a correction to the plasmon dispersion. The result is an accurate self-consistent and computationally efficient hydrodynamic description of the free-electron gas. A very accurate agreement with full quantum calculations is shown.

I. INTRODUCTION

Plasmonic nanosystems have enabled the possibility to macroscopically probe effects that are generally confined to the microscopic realm [1–8]. Nonlocal electron response [9–11] and quantum tunneling [12–15] have been experimentally observed in plasmonic systems characterized by subnanometer dielectric gaps. The advances of fabrication techniques allow one to control the features of such systems at the angstrom scale [16–18]. In this context, it becomes very important to develop simulation techniques to take into account quantum microscopic features at the scale of billions of atoms. Density functional theory (DFT) methods are generally unsuitable because their computational cost grows as fast as $O(N_e^3)$ such that their reach is limited to systems with few thousands of electrons [6]. Conversely, methods based on effective descriptions have also been proposed [19,20], although their applicability depends on *a priori* calculations usually relying on a different method and it is limited to the linear response regime.

A promising alternative is given by orbital-free techniques [21–23] where electron energy functionals are expressed in terms of the electron density, $n(\mathbf{r},t)$, rather than the single electronic orbitals. To this category belongs the *hydrodynamic theory* (HT), in which the quantum dynamics is solved via macroscopic observable quantities, such as n and the current density $\mathbf{J}(\mathbf{r},t)$ or the velocity $\mathbf{v}(\mathbf{r},t)$. The HT has a long history [24–26] and it has been applied to a variety of problems [27–30] including absorption of metallic nanoparticles (NPs) [31,32] and nonlinear optics [33–36].

Recently, the HT has vigorously reemerged in the context of nanoplasmonics [37–39], strongly fueled by the proliferation of self-assembling colloidal plasmonic structures [9,14,16–18]. Because of the complexity of the systems involved, however, the HT has usually been considered within the limit of the Thomas-Fermi (TF) approximation with the assumption of a constant ground density, neglecting essential effects such as electron spill-out and quantum tunneling. The TF-HT, however, can be greatly improved by adding a ∇n-dependent contribution—the von Weizsäcker (vW) correction—to the TF kinetic energy of the free-electron gas. In this way, a space-dependent ground density can be easily taken into

account. In conformity with the recent literature I will refer to this model to as the *quantum hydrodynamic theory* (QHT). A self-consistent approach based on the QHT coupled to Maxwell's equations was recently introduced by Toscano *et al.*, who applied it to show size-dependent blueshift in small noble metal nanowires [40]. Systematic comparisons of QHT with DFT results [41,42], however, pointed out that in order to describe well both near- and far-field features of plasmonic systems, one might need to sacrifice the self-consistency of the method [42]. A precise prediction of the fields near the surface is in fact extremely important for tunneling regimes and nonlinear applications. Moreover, in its present form the QHT does not take into account size-dependent broadening of the plasmonic resonances, although a recent effort in this direction [43] suggested the use of a density-dependent damping rate. It is worth noting that although the exact hydrodynamic form of the many-body time-dependent Schrödinger equation has been known (in a nonclosed form) for a long time [44], its actual implementation has been very difficult due to the fact that the functional dependence of the stress tensor on the density and the currents is still unknown. As for all orbital-free methods, the challenge is to find an appropriate approximate functional that correctly accounts for the electron gas total energy. In recent years, efforts in this direction have increased [45–50].

In this paper, I first show that the QHT equation in the limit of TF-vW approximation can be formally derived from the single-particle Kohn-Sham (KS) equation. This derivation clearly shows the degree of approximations that are made when using the QHT. As the second step, a correction of the form of a kinetic viscous tensor is introduced empirically in order to take into account Landau-damping effects. Moreover, because the QHT intrinsically describes both longitudinal and transverse fields, it is then possible to include in the Hamiltonian a current-dependent exchange-correlation (XC) vector potential. Such potential has been developed by Vignale and Kohn [51] in the context of the current density functional theory (CDFT). The peculiarity of this functional is that it has the form of a divergence of a viscoelastic stress tensor. The result is a self-consistent theory that can be applied to much larger scale problems compared to DFT techniques, with comparable accuracy. The theory correctly predicts size-dependent plasmon energies and broadening, as well as near-field properties. Application to NP dimers also shows good agreement with DFT calculations previously published, down to the tunneling regime.

[*]cristian.ciraci@iit.it

II. QUANTUM HYDRODYNAMIC EQUATION

The HT is formally exact solely for a single- or two-particle system in which the particles lay in one identical state, and in this case its equations can be easily derived from Schrödinger's equation [24]. Such a procedure cannot be applied for many-particle systems, and in this case the HT equations are usually approximated either by deriving the first N moments of the collisionless Boltzmann equations [52–54] or assuming a certain expression for the total energy of the system in a variational formulation [29,40,55]. Here, we would like to derive the QHT equations from the single-particle KS equation. In order to do so, let us consider a system of N_e noninteracting particles in the presence of an electromagnetic field generated by the scalar and vector potentials $v_e(\mathbf{r},t)$ and $\mathbf{A}_m(\mathbf{r},t)$, and in the presence of the XC potential energy $v_{\text{XC}}(\mathbf{r},t)$ and vector potential $\mathbf{A}_{\text{XC}}(\mathbf{r},t)$. The system is described by a set of time-dependent KS equations for the single orbitals $\varphi_j(\mathbf{r},t)$, $j = 1 \ldots N_e$:

$$i\hbar \frac{\partial \varphi_j}{\partial t} = \left[\frac{(i\hbar\boldsymbol{\nabla} - e\mathbf{A})^2}{2m} - ev_e + v_{\text{XC}} \right]\varphi_j, \qquad (1)$$

where $\hbar$ is the reduced Planck constant, m and e are the electron mass and charge (in absolute value), respectively, and $\mathbf{A} = \mathbf{A}_m + \mathbf{A}_{\text{XC}}$. The electromagnetic potentials are related to the usual electric and magnetic fields as $\mathbf{E} = -\frac{\partial \mathbf{A}_m}{\partial t} - \boldsymbol{\nabla} v_e$ and $\mathbf{B} = \boldsymbol{\nabla} \times \mathbf{A}_{\text{m}}$, respectively.

Without loss of generality we can write the complex eigenfunctions as $\varphi_j = \phi_j e^{i\chi_j}$ with $\phi_j(\mathbf{r},t)$ and $\chi_j(\mathbf{r},t)$ purely real functions of space and time [24]. Our goal is to express Eq. (1) as a function of the global macroscopic variables $n(\mathbf{r},t)$ and $\mathbf{J}(\mathbf{r},t)$, which are defined as

$$n = \sum_{j\in\text{occ}} \phi_j^2, \quad \mathbf{J} = -e \sum_{j\in\text{occ}} \phi_j^2 \mathbf{v}_j - \frac{ne^2}{m}\mathbf{A}, \qquad (2)$$

where the sum is performed over all occupied states and $\mathbf{v}_j = \frac{\hbar}{m}\boldsymbol{\nabla}\chi_j$. Multiplying Eq. (1) by φ_j^*, summing over the occupied states and separating the real part of the resulting equation gives, after using the definition of Eq. (2), the following equation:

$$\frac{\partial \mathbf{J}}{\partial t} = \frac{ne^2}{m}\mathbf{E} - \frac{e}{m}\mathbf{J} \times (\mathbf{B} + \boldsymbol{\nabla} \times \mathbf{A}_{\text{XC}})$$
$$+ \frac{ne}{m}\left(\boldsymbol{\nabla} v_{\text{XC}} - e\frac{\partial \mathbf{A}_{\text{XC}}}{\partial t}\right) + \frac{e}{m}\boldsymbol{\nabla} \cdot \boldsymbol{\Pi}, \qquad (3)$$

where the momentum flux tensor $\boldsymbol{\Pi}$ is given by

$$\Pi_{\mu\nu} = \frac{\hbar^2}{2m}\left(-\frac{\delta_{\mu\nu}}{2}\nabla^2 n + 2\sum_{j\in\text{occ}} \frac{\partial \phi_j}{\partial r_\mu}\frac{\partial \phi_j}{\partial r_\nu}\right)$$
$$+ m\sum_{j\in\text{occ}} \phi_j^2\left(v_{\mu,j} + \frac{e}{m}A_\mu\right)\left(v_{\nu,j} + \frac{e}{m}A_\nu\right), \quad (4)$$

with subscripts μ and ν spanning the Cartesian directions and $\delta_{\mu\nu}$ being the Kronecker delta.

It is useful to extract from the sums in Eq. (4) the known quantities. To do so, let us write the single orbitals as the difference, $\tilde{\phi}_j$, with respect to an average orbital $\phi = \sqrt{\frac{n}{N_e}}$,

so that we have $\phi_j = \phi + \tilde{\phi}_j$. Analogously, for the velocities we have $\mathbf{v}_j = \mathbf{v} + \tilde{\mathbf{v}}_j$, where $\mathbf{v} = \mathbf{J}/(-en) - e\mathbf{A}/m$ (note that by construction $\sum_{j\in\text{occ}} \phi_j^2 \tilde{\mathbf{v}}_j = 0$). After the new definitions, Eq. (3) can be written as

$$\frac{\partial \mathbf{J}}{\partial t} = \frac{ne^2}{m}\mathbf{E} - \frac{e}{m}\mathbf{J} \times (\mathbf{B} + \boldsymbol{\nabla} \times \mathbf{A}_{\text{XC}})$$
$$+ \frac{ne}{m}\left(\boldsymbol{\nabla} v_{\text{XC}} - e\frac{\partial \mathbf{A}_{\text{XC}}}{\partial t}\right) + \frac{ne}{m}\boldsymbol{\nabla}\frac{\delta T_{\text{W}}}{\delta n}$$
$$+ \frac{1}{e}\left(\frac{\mathbf{J}}{n}\boldsymbol{\nabla} \cdot \mathbf{J} + \mathbf{J} \cdot \boldsymbol{\nabla}\frac{\mathbf{J}}{n}\right) + \frac{e}{m}\boldsymbol{\nabla} \cdot \boldsymbol{\Pi}', \qquad (5)$$

where $\frac{\delta T_{\text{W}}}{\delta n} = \frac{\hbar^2}{8m}\left(\frac{\boldsymbol{\nabla} n \cdot \boldsymbol{\nabla} n}{n^2} - 2\frac{\nabla^2 n}{n}\right)$ is the vW kinetic potential, and the remaining part of the momentum flux tensor is

$$\Pi'_{\mu\nu} = \frac{\hbar^2}{m}\sum_{j\in\text{occ}}\frac{\partial \tilde{\phi}_j}{\partial r_\mu}\frac{\partial \phi}{\partial r_\nu} + \frac{\partial \phi}{\partial r_\mu}\frac{\partial \tilde{\phi}_j}{\partial r_\nu} + \frac{\partial \tilde{\phi}_j}{\partial r_\mu}\frac{\partial \tilde{\phi}_j}{\partial r_\nu}$$
$$+ m\sum_{j\in\text{occ}} \phi_j^2 \tilde{v}_{\mu,j}\tilde{v}_{\nu,j}. \qquad (6)$$

It is worth noting that no approximations have been made up to this point. In particular, the vW potential has been exactly derived from Eq. (1). This allows one to exactly define the prefactor λ that usually precedes the vW term. This number varies in the literature from $1/9$ to 1. It is clear from the presented derivation that the right choice should be $\lambda = 1$ as already suggested in previous publications [41,42] by direct comparisons with DFT results.

Moreover, for the simple case of $N_e = 2$ (single orbital) it easy to show that $\Pi'_{\mu\nu} = 0$. In fact because there is one occupied orbital $\phi_1 = \sqrt{n/2}$, the electrons move in phase, hence $\tilde{\mathbf{v}}_1 = 0$. Equation (5) is then an exact hydrodynamic description of the two-electron system. Solving this equation would give the exact same result as Eq. (1). In general, however, $\Pi'_{\mu\nu} \neq 0$ and Eq. (5) cannot be solved without knowing the single orbitals ϕ_j.

Our next step is then finding an approximation for $\Pi'_{\mu\nu}$ that will allow its evaluation without having to solve for the orbitals ϕ_j. Let me anticipate that such approximation is in fact the TF contribution to the kinetic energy. In particular, I will show that $\boldsymbol{\nabla} \cdot \boldsymbol{\Pi}' \simeq n\boldsymbol{\nabla}\frac{\delta T_{\text{TF}}}{\delta n}$, where $T_{\text{TF}} = c_{\text{TF}} n^{5/3}$, with $c_{\text{TF}} = \frac{\hbar^2}{m}\frac{3}{10}(3\pi)^{2/3}$.

Since we are interested in describing structures that are constituted by a large number of electrons, in first approximation we can consider the electronic system as a homogeneous electron gas whose orbitals are $\varphi_{\mathbf{k}} = \frac{e^{i\mathbf{k}\cdot\mathbf{r}}}{V^{1/2}}$, with V the occupied volume in real space. It is easy to identify $\hbar\mathbf{k} = m\tilde{\mathbf{v}}_j$ (without the net contribution induced by the external fields), so that the sum over j becomes a sum of $\mathbf{k}$:

$$\frac{\partial \Pi'_{\mu\nu}}{\partial r_\nu} \simeq m\frac{\partial}{\partial r_\nu}\sum_{j\in\text{occ}} \phi_j^2 \tilde{v}_{\mu,j}\tilde{v}_{\nu,j} \simeq \frac{2\hbar^2}{mV}\frac{\partial}{\partial r_\nu}\sum_{\mathbf{k}\in\text{occ}} k_\mu k_\nu, \quad (7)$$

where the first sum in Eq. (6) is zero because the amplitudes associated to the orbitals $\varphi_{\mathbf{k}}$ are constant. Note, however, that even if every term in Eq. (7) seems to be constant, taking the divergence of the sum will not give equally zero, because, as will be clear later, the number of occupied states will depend on the local density $n(\mathbf{r})$. Since there are many occupied states,

we can replace as usual the sum by an integral:

$$\frac{2\hbar^2}{mV}\frac{\partial}{\partial r_\nu}\sum_{\mathbf{k}\in\text{occ}}k_\mu k_\nu$$

$$\simeq \frac{\hbar^2}{m4\pi^3}\frac{\partial}{\partial r_\nu}\int_0^{k_\text{F}}k^4 dk\int_0^\pi\int_0^{2\pi}\hat{k}_\mu\hat{k}_\nu\sin\theta\,d\theta\,d\phi, \quad (8)$$

where we used $dn = \frac{V}{8\pi^3}d\mathbf{k}$ and $k_\text{F}(\mathbf{r}) = (3\pi^2 n)^{1/3}$. Evaluating the integrals gives

$$\boldsymbol{\nabla}\cdot\boldsymbol{\Pi}' \simeq \frac{\hbar^2}{m\pi^2}\frac{1}{15}\frac{\partial}{\partial r_\nu}\left(\delta_{\mu\nu}k_\text{F}^5\right) = \frac{10}{9}c_\text{TF}n^{2/3}\boldsymbol{\nabla}n. \quad (9)$$

It is easy now to show that the last term in the previous equation is exactly equal to $n\boldsymbol{\nabla}\frac{\delta T_\text{TF}}{\delta n}$, as was anticipated.

III. BEYOND THE THOMAS-FERMI KINETIC ENERGY

The derivation performed in the previous section demonstrates that the error committed using the QHT is solely given by the approximation (9). We can write then

$$\boldsymbol{\nabla}\cdot\boldsymbol{\Pi}' = n\boldsymbol{\nabla}\frac{\delta T_\text{TF}}{\delta n} + \boldsymbol{\nabla}\cdot\boldsymbol{\Pi}'', \quad (10)$$

with $\boldsymbol{\Pi}''$ being a tensor that accounts for a correction to the TF potential. This tensor can be further decomposed in a contribution P that depends on the instantaneous density, as well as a dynamical term Ω:

$$\boldsymbol{\Pi}'' = \text{P}(n) + \Omega(n,\omega). \quad (11)$$

P is important in the static case since it guarantees the calculation of the exact ground-state density, while Ω ensures a proper frequency-dependent response. Unfortunately it is still a major issue being able to derive good expressions for P and Ω without knowing the exact orbitals [56–58]. In this paper I will focus on the dynamical component Ω and consider P = 0 for simplicity.

An important effect due to Ω is the broadening of the plasmonic resonance in bounded systems, such as metallic nanoparticles. In particular, the broadening is the result of exciting single particles into electron-hole pairs. In fact, the myriad of states existing at the surface of small particles provides a broad range of possible transitions that translate into a broadening of the collective plasmon resonance. In the HT electrons are assumed to lay in identical states and single-particle excitations cannot be exactly taken into account.

It is possible to assume, however, that the broadening of the collective resonance is due to the increase of effective collisions in the electron gas. These new collisions may be thought intuitively as the result of the different phase velocity between electrons in different states. An expression for Ω within the HT has been proposed by Tokatly, who derived a generalized HT by expanding the kinetic equation for the distribution function to high-order moments [53]. Tokatly obtained an expression of the form

$$\Omega_{\mu\nu} = -\sigma_{\mu\nu}^{(k)} = -\eta_k\left(\frac{\partial v_\mu}{\partial r_\nu} + \frac{\partial v_\nu}{\partial r_\mu} - \frac{2}{3}\delta_{\mu\nu}\boldsymbol{\nabla}\cdot\mathbf{v}\right), \quad (12)$$

where η_k is a phenomenological parameter that is in general a function of the density n. $\sigma_{\mu\nu}^{(k)}$ has the form of a viscous stress

tensor [53] and since it depends only on the induced velocity $\mathbf{v}$ it represents a dynamical correction to the kinetic energy functional. In Tokatly's theory the correction in Eq. (12) was derived for a homogeneous electron gas and it is limited to low frequencies; here it is assumed that such expression holds also at high frequencies to account for the *extra* collisions due to the presence of surface states. This assumption is supported by direct comparison to TD-DFT results in Sec. V.

It can be useful to regroup the total force exerted on the volume element due to the kinetic energy as

$$\mathbf{F} = -n\boldsymbol{\nabla}\left(\frac{\delta T_\text{TF}[n]}{\delta n} + \frac{\delta T_\text{W}[n,\boldsymbol{\nabla}n]}{\delta n}\right) + \boldsymbol{\nabla}\cdot\sigma^{(k)}. \quad (13)$$

It is interesting to notice that in the limit of a uniform electron density, Eq. (13) reduces to the generalized nonlocal term presented in Ref. [59], with an extra contribution proportional to $\nabla^2\mathbf{J}$, in addition to the term $\boldsymbol{\nabla}\boldsymbol{\nabla}\cdot\mathbf{J}$. The main difference, however, is that the authors of Ref. [59] attribute such correction to a somewhat arguable diffusion mechanism, rather than a much more intuitive viscouslike behavior of the electron gas.

IV. CURRENT-DEPENDENT XC POTENTIAL

It remains now to give an explicit expression for the XC potentials. For the scalar potential v_XC the usual local density approximation is assumed [60]. That is, we approximate the XC scalar potential v_XC as a function of the instantaneous local density:

$$v_\text{XC}[n(\mathbf{r},t)] = \frac{\delta}{\delta n}[n\varepsilon_\text{XC}(n)], \quad (14)$$

where $\varepsilon_\text{XC} = \varepsilon_x + \varepsilon_c$ is the XC energy per particle of a homogeneous electron gas with density n and the exchange and correlation energies are defined, respectively, as [38]

$$\varepsilon_x(n) = -(E_h a_0)\frac{3}{4}\left(\frac{3}{\pi}n\right)^{1/3},$$

$$\varepsilon_c(n) = E_h\begin{cases}a_c\ln(r_s) + b_c + c_c r_s\ln(r_s) + d_c r_s, & r_s < 1 \\ \frac{\alpha}{1+\beta_1\sqrt{r_s}+\beta_2 r_s}, & r_s \geqslant 1,\end{cases}$$

$$(15)$$

where $E_h = \frac{\hbar^2}{ma_0^2}$ is the Hartree energy, a_0 is the Bohr radius, $a_0 r_s = \left(\frac{3}{4\pi n}\right)^{1/3}$ is the Wigner-Seitz radius, and the coefficients are $a_c = 0.0311$, $b_c = -0.048$, $c_c = 0.002$, $d_c = -0.0116$, $\alpha = -0.1423$, $\beta_1 = 1.0529$, and $\beta_2 = 0.3334$. Equation (15), as well as other formulas in this paper, are in S.I. units; expressions in atomic units (a.u.) can also be easily obtained by considering that $E_h = a_0 = m = \hbar = 1$.

The XC potential, however, is an intrinsically nonlocal functional of the density, namely, it does not admit a gradient expansion in n without sacrificing some basic symmetries [51,61]. Fortunately, Vignale and Kohn have shown in the context of CDFT that a local gradient expansion is still possible in terms of $\mathbf{J}$, and have provided an explicit approximated expression for the XC vector potential $\mathbf{A}_\text{XC}$ [51]. It was later shown that the XC vector potential can be arranged into a more intuitive form [61], so that it is expressed as the divergence of

the viscoelastic stress tensor, namely,

$$\frac{\partial \mathbf{A}_{\mathrm{XC}}}{\partial t} = \frac{1}{en} \nabla \cdot \sigma^{(xc)}, \tag{16}$$

where $\sigma^{(xc)}$ is the classical viscoelastic stress tensor:

$$\sigma_{\mu\nu}^{(xc)} = \tilde{\eta}_{xc}\left(\frac{\partial v_\mu}{\partial r_\nu} + \frac{\partial v_\nu}{\partial r_\mu} - \frac{2}{3}\delta_{\mu\nu}\nabla \cdot \mathbf{v}\right) + \tilde{\xi}_{xc}\delta_{\mu\nu}\nabla \cdot \mathbf{v}, \tag{17}$$

with $\tilde{\eta}_{xc}$ and $\tilde{\xi}_{xc}$ generalized complex viscosities that depend on the density n and the frequency ω, and can be related to the $k \to 0$ limit of the XC longitudinal and transverse kernel functions $f_{\mathrm{XC,L(T)}}(\omega, \mathbf{k})$ [61]. The caveat is that the kernel functions are not known exactly, although several interpolation formulas have been developed [62–65].

In this work the interpolation proposed by Conti and Vignale (CV) is used [66]. Let us write the complex viscosities as

$$\tilde{\eta}_{xc}(\omega, \mathbf{r}) = \eta_{CV}(\mathbf{r}) - \frac{\mu_{CV}(\mathbf{r})}{i\omega},$$

$$\tilde{\xi}_{xc}(\omega, \mathbf{r}) = \zeta_{CV}(\mathbf{r}) - \frac{K_{CV}(\mathbf{r})}{i\omega}, \tag{18}$$

where all the coefficients are real quantities independent of the frequency, whose interpolation formulas in the CV approximation are

$$\eta_{\mathrm{CV}}(\mathbf{r}) = \hbar\left(60r_s^{-3/2} + 80r_s^{-1} - 40r_s^{-2/3} + 62r_s^{-1/3}\right)^{-1}n,$$

$$K_{\mathrm{CV}}(\mathbf{r}) = (E_h)n^2\frac{d^2}{dn^2}[n\varepsilon_{\mathrm{XC}}(n)],$$

$$\zeta_{\mathrm{CV}}(\mathbf{r}) = 0,$$

$$\mu_{\mathrm{CV}}(\mathbf{r}) = E_h\left(ar_s^{-2} + br_s^{-1} + \frac{c-b}{r_s+20}\right)n, \tag{19}$$

with $a = \frac{1}{5}\left(\frac{9\pi}{4}\right)^{2/3}$, $b = \frac{1}{10}\left(\frac{3}{2\pi}\right)^{2/3}$, and $c = 0.12$.

Expression (17) with the complex coefficients (18) is only valid if a time-harmonic dependence is considered. In general, however, the tensor (17) can be decomposed into a viscous and an elastic term so that we have

$$\sigma_{\mu\nu}^{(xc)} = \eta_{\mathrm{CV}}\left(\frac{\partial v_\mu}{\partial r_\nu} + \frac{\partial v_\nu}{\partial r_\mu} - \frac{2}{3}\delta_{\mu\nu}\nabla \cdot \mathbf{v}\right)$$

$$+ \mu_{\mathrm{CV}}\left(\frac{\partial u_\mu}{\partial r_\nu} + \frac{\partial u_\nu}{\partial r_\mu} - \frac{2}{3}\delta_{\mu\nu}\nabla \cdot \mathbf{u}\right) + K_{\mathrm{CV}}\delta_{\mu\nu}\nabla \cdot \mathbf{u}, \tag{20}$$

with $\mathbf{u}$ being the displacement vector such that $\dot{\mathbf{u}} = \mathbf{v}$.

Equation (20) is very similar to Eq. (12) and does not add any degree of complexity to the problem. The XC vector potential provides a further dissipation mechanism

contributing to the lifetime of collective excitations [67–69], although it is usually small compared to the contribution of the kinetic component. More importantly, Eq. (20) adds an elasticlike behavior to the electron gas (not present in the viscouslike kinetic term) that partially affects the position of the collective resonance.

V. RESULTS

Before showing some applications of the model obtained, let us summarize all the elements into a single equation. By combining Eq. (5) with Eqs. (11) and (12) and Eq. (20) we obtain

$$\frac{\partial \mathbf{J}}{\partial t} = \frac{ne^2}{m}\mathbf{E} + \frac{ne}{m}\nabla\frac{\delta G}{\delta n} + \frac{e}{m}\nabla \cdot \sigma^{(kxc)}$$

$$+ \frac{1}{e}\left(\frac{\mathbf{J}}{n}\nabla \cdot \mathbf{J} + \mathbf{J} \cdot \nabla\frac{\mathbf{J}}{n}\right) - \frac{e}{m}\mathbf{J} \times (\mathbf{B} + \nabla \times \mathbf{A}_{\mathrm{XC}}), \tag{21}$$

where $\frac{\delta G}{\delta n} = \frac{\delta T_{\mathrm{TF}}}{\delta n} + \frac{\delta T_{\mathrm{W}}}{\delta n} + v_{\mathrm{XC}}$, and $\sigma^{(kxc)} = \sigma^{(k)} + \sigma^{(xc)}$ is the viscoelastic kinetic-XC tensor. Equation (21) coupled to Maxwell's equations describes self-consistently the linear and nonlinear electromagnetic response of a free-electron gas. A similar equation can also be obtained from Euler's equation [33,35] where the total internal energy term is limited to a scalar pressure (i.e., TF approximation) and the viscoelastic tensor is neglected. We can identify, in fact, on the right-hand side of Eq. (21), the Coulomb force term ($\propto n\mathbf{E}$), the convective terms ($\propto \mathbf{J}\nabla \cdot \mathbf{J}$ and $\mathbf{J} \cdot \nabla\mathbf{J}$), and the Lorentz force term ($\propto \mathbf{E} \times \mathbf{B}$). These terms are important in the study of the nonlinear optical response of metallic systems [33,35,36]. In addition to previously published results, Eq. (21) introduces several new (nonlinear) terms that are hidden in the total internal energy expression, which is in general a nonlinear function of the electron density and in the viscoelastic term, aside from the Lorentz-like term associated to the XC vector. These terms are expected to be important in the nonlinear response of nanogap plasmonic systems [16,70,71].

More importantly, the viscoelastic term contains an effective k-dependent mechanism for dissipating energy. This is associated to an increase of electron-electron collisions near the particle surface where, in fact, the gradient of the velocity is larger. This term is not only expected to strongly impact the spectral width of linear response resonances but also the optical nonlinear signals generated at the metal surface.

It is worth noting that while the XC component of the viscoelastic tensor was explicitly given in Eqs. (19) and (20), the coefficient η_k associated with the kinetic viscous tensor is yet to be specified. Finding a rigorous expression for η_k as a function of the density n is a very challenging problem and a more rigorous study is remitted to future works. For simplicity, in this paper, let us assume that $\eta_k \propto \eta_{\mathrm{CV}}$. It is found that the particular choice of $\eta_k = 14\eta_{\mathrm{CV}}$ gives a great degree of predictability in terms of near- and far-field properties, as is shown below.

As a first application of Eq. (21), let us consider the linear optical response of single jellium nanospheres. By linearizing Eq. (21), coupling it to Maxwell's equations, and remembering that $\partial \mathbf{P}/\partial t = \mathbf{J}$ and $\mathbf{v} = \mathbf{J}/(-en)$, we obtain in the frequency
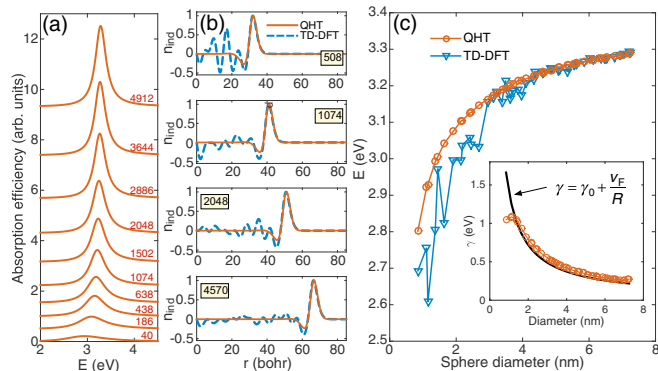
FIG. 1. Properties of jellium spheres ($r_s = 4$ a.u.) of different sizes: (a) absorption cross-section; (b) imaginary part of the normalized induced charge density; (c) plasmon resonance as a function of the sphere diameter; in the inset, the broadening of the resonance for QHT. Peak positions and widths were calculated by fitting the spectra with a Lorentzian-shaped function; TD-DFT data are taken from Ref. [42].

domain the following system of equations:

$$\nabla \times \nabla \times \mathbf{E} - \frac{\omega^2}{c^2}\mathbf{E} = \omega^2 \mu_0 \mathbf{P},$$

$$-\frac{n_0 e}{m}\nabla\left(\frac{\delta G}{\delta n}\right)_1 + \frac{e}{m}\nabla \cdot \sigma^{(kxc)} - (\omega^2 + i\omega\gamma)\mathbf{P} = \frac{n_0 e^2}{m}\mathbf{E},$$

$$(22)$$

where $n_0(\mathbf{r})$ is the equilibrium density, μ_0 and c are the magnetic permeability and the speed of light in vacuum, respectively, $\left(\frac{\delta G}{\delta n}\right)_1$ is the first-order term for the potential (whose explicit expressions can be found in Ref. [42]). In writing the second Eq. (22) the phenomenological damping rate γ has been introduced in order to take into account losses occurring in the bulk regions.

The ground state n_0 can be calculated self-consistently (see Appendix A 1 for details) by solving the following differential equation [40]:

$$\nabla^2\left(\frac{\delta G[n]}{\delta n}\right)_{n=n_0} + \frac{e^2}{\epsilon_0}(n_0 - n^+) = 0, \qquad (23)$$

where ϵ_0 is the electric permittivity and n^+ is the homogeneous ion density. Note that since $\sigma^{(kxc)}$ affects only the dynamical response, Eq. (23) and the properties of its solution n_0 remain unchanged with respect to Ref. [42].

The system of Eqs. (22) and Eq. (23) are numerically solved with a commercial software based on the finite-element method, COMSOL MULTIPHYSICS [72]. In particular, the 2.5D technique [73] has been used, which allows one to efficiently compute absorption spectra for axis symmetric structures (see Appendix A 2).

Absorption spectra for different jellium Na ($r_s = 4$ a.u.) nanospheres are shown in Fig. 1(a). The first thing to notice is that as the particle size shrinks the broader are their plasmonic resonances. One important difference with previous QHT results [42] is the absence of higher energy resonances. These resonances are the analog of Rydberg states for atoms. They are associated with very delocalized states and are numerically

affected by the finiteness of the simulation domain size. With the introduction of the viscosity, these states are no longer supported as would be expected for jellium spheres [39].

In Fig. 1(b) the QHT-induced charge densities corresponding to plasmon energy are compared to the time-dependent (TD) DFT results. Although oscillations appearing in the TD-DFT case in the bulk region are not reproduced, the main induced peak is very well described by the QHT. Note that this is not necessarily the case for the approach used in Ref. [43]. Because $\gamma \propto n_0^{-5/6}$ diverges near the particle surface, the induced density results *prematurely* damped at the surface.

In Fig. 1(c) the plasmon resonances obtained with the present QHT model are compared against TD-DFT results [42], for NP diameters D ranging from $\sim$0.85 to $\sim$7.25 nm ($N_e = 8$ to $N_e = 5032$). For $D > 3$ nm ($N_e > 398$) QHT reproduces DFT plasmon energies with great accuracy, with QHT resonances marking almost exactly the mean trajectory of DFT data. Also striking is the comparison of the broadening of the resonance shown in the inset. The reference curve in this case is given by the known formula [74] $\gamma = \gamma_0 + v_F/R$ where v_F is the Fermi velocity for the homogeneous electron gas and $R = D/2$. The agreement is very good for all the diameters except the smallest ones for which the analytical formula is not expected to hold.

A. Nanoparticle dimer

Another important system to consider is the NP dimer. As the distance between two closely spaced NPs reduces, four different effects come simultaneously into play [1,6,9,12]: (i) hybridization of the plasmonic modes; (ii) nonlocality character of the optical response; (iii) broadening of the resonance, which is intrinsically due to nonlocal absorption (since the size of the spheres remains unchanged); and (iv) tunneling effects due to the bonding of the electron density tails. The NP dimer represents then an important test of the QHT presented here.

Let us consider a dimer of Na spheres of $D \simeq 3$ nm ($N_e = 398$) and separated by a distance g that goes from 2 to 0 nm. The dimer is excited by a plane wave propagating orthogonally to the dimer axis whose electric field is polarized along z, as depicted in Fig. 2(a). The ground-state charge density has been self-consistently calculated using Eq. (23) for each value of the distance g. The map of Fig. 2(b) shows the absorption spectrum of the dimer as a function of the gap size. As the gap shrinks the plasmon resonance undergoes a redshift up to the point ($g \simeq 0.4$ nm) where tunneling effects kick in and the resonance broadens and the shift pushes back to higher energies. Note that without the kinetic-XC viscosity the QHT would have predicted an unnoticeable broadening.

In Fig. 2(c) are reported the equilibrium charge density n_0, the induced density n_1, and the electric field norm distribution, respectively, for three critical situations labeled in the map [in Fig. 2(b)]. These results can be directly compared to results of Ref. [75] in which TD-DFT calculations for the same jellium Na dimer are reported. It can be seen that all quantities are well reproduced. It is worth noting that in DFT there is no intrinsic broadening mechanism for each spectral line and a phenomenological value of γ (usually much larger than the bulk value) has to be taken into account in order to produce a
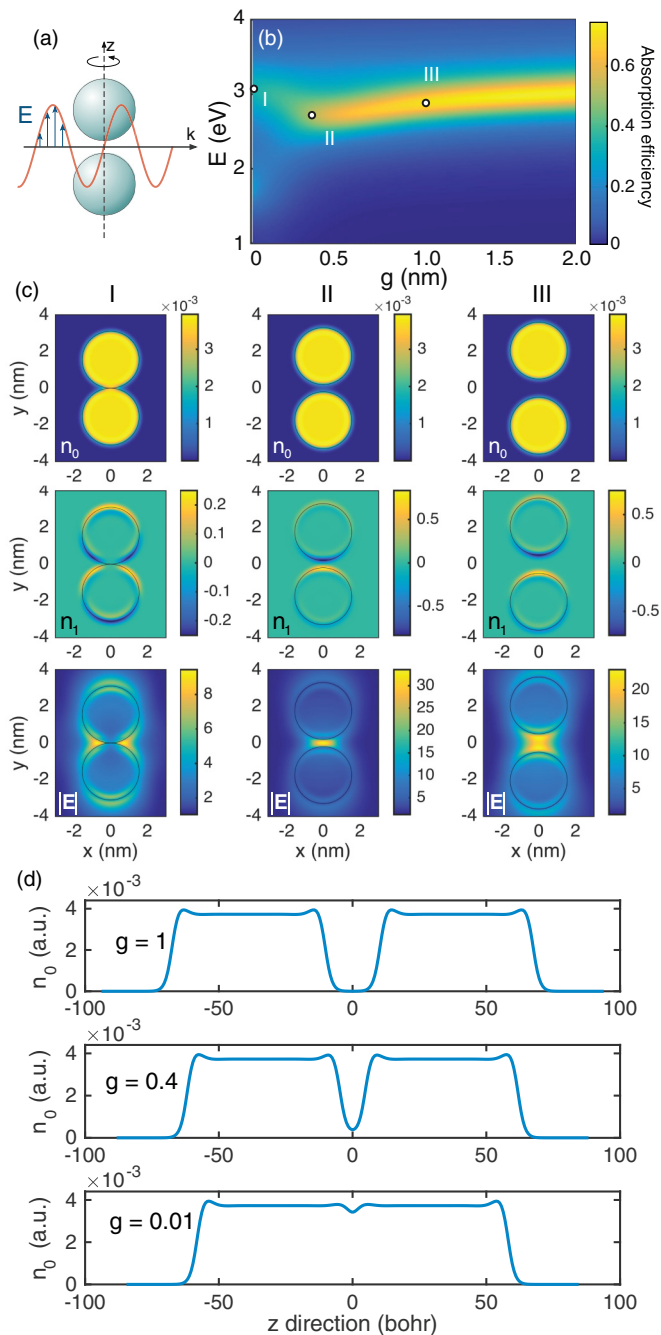
FIG. 2. Dimer of Na spheres constituted by $N_e = 398$ electrons each. (a) Scheme of the system; (b) absorption efficiency spectra as a function of the interparticle distance g; (c) near-field properties corresponding to the points depicted in (b) ($g = 1.0, 0.4, 0$ nm). The densities n_0 and n_1 are in atomic units, while $|\mathbf{E}|$ is normalized to the incident field amplitude. (d) Equilibrium density taken along the dimer axis at distances $g = 1.0, 0.4, 0.01$ nm.
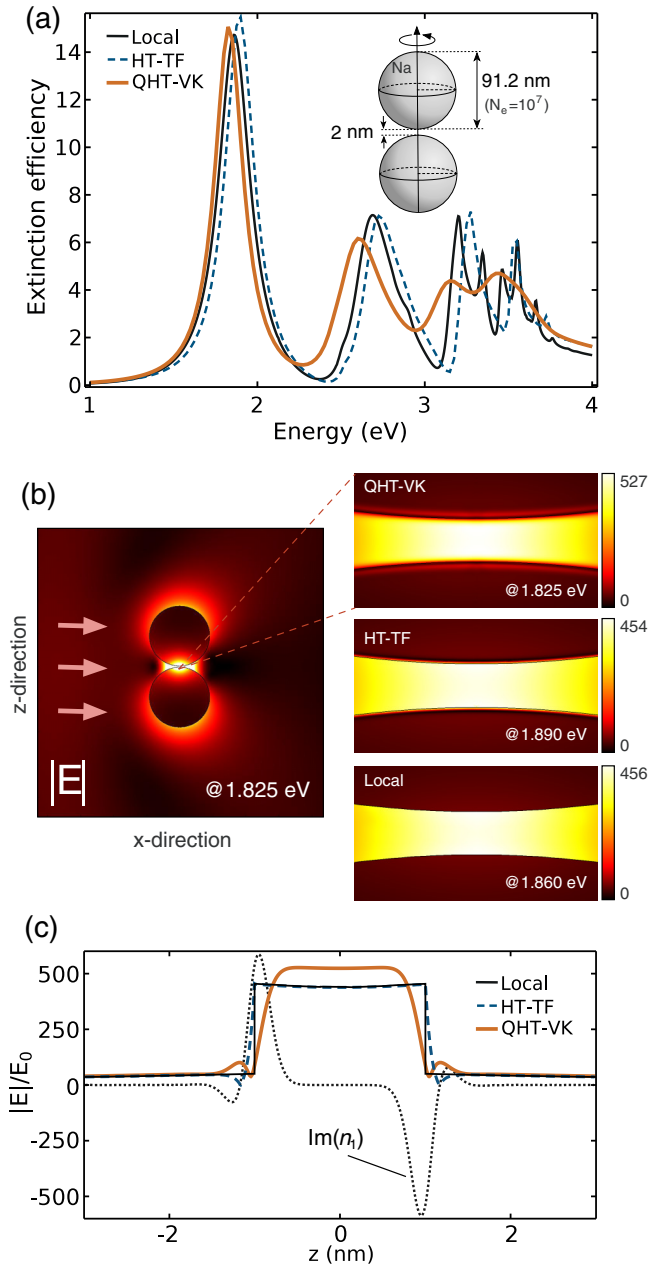

FIG. 3. Properties of a dimer of Na spheres constituted by $N_e = 10^7$ electrons each, placed at a distance of 2 nm. In (a), extinction spectra obtained using different methods. The maps in (b) depict the field enhancement around the structure, with a magnification of the gap region shown for each method. (c) Electric field norm along the gap for the various models. The imaginary part of the induced charge density for the QHT is also plotted.

B. A "macroscopic" system

In order to show the full potential of the QHT method let us consider a structure whose size makes it unapproachable by DFT techniques. Let us consider a dimer of Na spheres constituted by $N_e = 10^7$ electrons each (diameter of $\sim$91.2 nm) placed at a distance of 2 nm as depicted in the inset of Fig. 3(a). The QHT calculation is compared to local response and HT-TF calculations. As would be expected, the energy of the main plasmonic peak is slightly redshifted with respect to fully

continuous spectrum. In Fig. 2(d) the equilibrium density n_0 taken along the dimer axis for gaps approaching and entering the tunneling regime is reported. It can be clearly seen for the smallest gap that the resulting density is not simply a sum of the single-particle densities as would be expected.

classical calculations. On the contrary, the HT-TF predicts a slight blueshift.

Figure 3(b) shows the different near-field features in the region nearby the gap and the relative maximum field enhancement. It is interesting to notice that while the local and HT-TF calculations predict the same amount of maximum field enhancement with respect to the incident amplitude $|\mathbf{E}|/E_0 \simeq 455$, the QHT predicts a $\sim$15% stronger field inside the gap region, $|\mathbf{E}|/E_0 = 527$ as is highlighted in Fig. 3(c). This result might be surprising, since the presence of nonlocal or quantum effects is usually associated to a detrimental effect on the field enhancement [6,9,15]. The result is, however, in agreement with previously published systematic studies on closely spaced nanowires [8]. Teperik *et al.* have shown, in fact, that by changing the effective gap size it is possible to retrieve the spectral features of various methods. In particular, for local or TF-FT models to reproduce TD-DFT results for Na coupled nanowires, it is necessary to reduce the effective gap size. This is in accord with an increase of the maximum fields since a smaller gap would correspond to a higher local field enhancement. Teperik and co-workers found that for small wires the variation of the gap is of the order of 2δ, where $\delta \simeq 0.9$ Å. Although this would seem a small correction, I have verified that the increase in the field enhancement corresponding to the local model in which the gap is reduced by 2δ gives similar results as the QHT model for the system considered.

It is worth noting that the increase of the local field enhancement observed in Na jellium sphere dimers might not be generally valid, in particular for noble metal systems. For silver and gold, in fact, the effective screening charge is inside the jellium edge and the effective gap size might result as larger than the actual separation between the jellium edges [8].

VI. CONCLUSION

I have presented a QHT model that is able to accurately and self-consistently describe far-field and near-field properties of plasmonic systems in most extreme conditions. This model represents a general theory that is also valid in the nonlinear regime [61] and could be used for the investigation of optical nonlinear surface effects.

Although the approximation introduced for the kinetic stress tensor lacks an analytical microscopic derivation, the model offers a great degree of predictability, even in situations where quantum tunneling cannot be neglected, and it might play an important role in the development of the field.

Finally, I believe this work offers a valid and efficient solution for studying in detail electron dynamics of mesoscopic structures. The computational scaling in fact does not depend on the number of electrons N_e in the system (as in DFT) but rather on the complexity of the equilibrium density function which is being discretized. The QHT self-consistent density results are constant in the bulk region and only fast-varying at the metal boundaries. The computational cost would then scale in principle as a function of the boundary area, rather than the volume, providing an extremely efficient computational tool. This gives access to an unparalleled regime of light-matter interactions, which in turn might lead to novel and unexploited effects.

APPENDIX: NUMERICAL IMPLEMENTATION

1. Ground-state density

The static quantum hydrodynamic equation for the calculation of the ground density can be obtained from Eq. (21):

$$\nabla\left(\frac{\delta G[n]}{\delta n}\right)_{n=n_0} - e\mathbf{E}_0 = 0, \tag{A1}$$

where the subscript "0" indicates the *zero* frequency dependence. In order to be solved, this equation must be coupled to Gauss's law:

$$\nabla \cdot \mathbf{E}_0 = -\frac{e}{\varepsilon_0}(n_0 - n^+), \tag{A2}$$

where n^+ is the positive background charge, which is assumed to be constant inside the jellium sphere while it abruptly drops to zero outside the jellium edge. By taking the divergence of Eq. (A1) and using Eq. (A2) it is possible to obtain one single nonlinear differential equation:

$$\nabla^2\left(\frac{\delta G[n]}{\delta n}\right)_{n=n_0} + \frac{e^2}{\varepsilon_0}(n_0 - n^+) = 0. \tag{A3}$$

I solved this equation using a commercially available software based on the finite-element method (FEM), COMSOL MULTIPHYSICS [72]. It was found that convergence is more easily achieved by solving for the transformed variable $\xi = \sqrt{n_0}$, and since FEM techniques usually require one to write the differential problem into its weak form, by multiplying Eq. (A3) by the test function $\tilde{\xi}$ and integrating over the simulation domain Ω we obtain the following weak form:

$$\int_{\Omega} -\nabla\left(\frac{\delta G[\xi^2]}{\delta n}\right)_{\xi=\sqrt{n_0}} \cdot \nabla\tilde{\xi} + \frac{e^2}{\varepsilon_0}(\xi^2 - n^+)\tilde{\xi}\,dV = 0, \tag{A4}$$

where it is assumed zero contribution from the integral over the boundaries of the domain Ω. I solve Eq. (A4) iteratively using COMSOL's built-in nonlinear solver based on Newton's method. The initial guess value for n_0, in the case of a single sphere, was taken of the form $n_0(r) = \frac{n_b}{1+\exp(\kappa r - R)}$ with n_b the bulk density and R the radius of the sphere. For the dimer case I used the solution for the single sphere and slowly reduced the gap from $g = 2$ to 0.01 nm.

2. The linear response

For the linear response I solved the system of Eqs. (22) in the main text. In particular, I used for the polarization equation the following weak expression:

$$\int_V \frac{e}{m}\left(\frac{\delta G}{\delta n}\right)_1 (n_0\nabla \cdot \tilde{\mathbf{P}} + \nabla n_0 \cdot \tilde{\mathbf{P}}) + \frac{i\omega}{m}\sum_{\mu,\nu}\sigma_{\mu\nu}\frac{\partial \tilde{P}_\mu}{\partial r_\nu}$$

$$+ \left[(-\omega^2 + i\omega\gamma)\mathbf{P} - \frac{ne^2}{m}\mathbf{E}\right] \cdot \tilde{\mathbf{P}}\,dV = 0, \tag{A5}$$

where $\tilde{\mathbf{P}}$ is the test function and the viscoelastic stress tensor σ as a function of the equilibrium density n_0 and the polarization vector $\mathbf{P}$ is

$$\sigma_{\mu\nu} = \tilde{\eta}\left[\frac{\partial}{\partial r_\nu}\left(\frac{P_\mu}{n_0}\right) + \frac{\partial}{\partial r_\mu}\left(\frac{P_\nu}{n_0}\right) - \frac{2}{3}\delta_{\mu\nu}\frac{\partial}{\partial r_l}\left(\frac{P_l}{n_0}\right)\right] + \tilde{\zeta}\delta_{\mu\nu}\frac{\partial}{\partial r_l}\left(\frac{P_l}{n_0}\right). \tag{A6}$$

Note that because we distributed the derivatives to the test functions $\tilde{\mathbf{P}}$ we do not need to evaluate the gradient of the functional $\left(\frac{\delta G}{\delta n}\right)_1$, nor the divergence of the viscoelastic stress tensor σ. Explicit expressions for $\left(\frac{\delta G}{\delta n}\right)_1$ can be found in Ref. [42].

In order to take advantage from the symmetry of the geometry, I have implemented our equations assuming an azimuthal dependence of the form $e^{-im\phi}$ with $m \in \mathbb{Z}$. That is, for a vector field $\mathbf{V}$, we have $\mathbf{V}(\rho,\phi,z) = \sum_{m\in\mathbb{Z}} \mathbf{V}^{(m)}(\rho,z)e^{-im\phi}$. Maxwell's equation and the polarization equation are written assuming the following definitions:

$$\nabla \cdot \mathbf{V}^{(m)} \equiv \left(\frac{1}{\rho} + \frac{\partial}{\partial\rho}\right)V_\rho^{(m)} - \frac{im}{\rho}V_\phi^{(m)} + \frac{\partial V_z^{(m)}}{\partial z},$$

$$\nabla \times \mathbf{V}^{(m)} \equiv \hat{\rho}\left(-\frac{\partial V_\phi^{(m)}}{\partial z} - i\frac{m}{\rho}V_z^{(m)}\right) + \hat{\phi}\left(\frac{\partial V_\rho^{(m)}}{\partial z} - \frac{\partial V_z^{(m)}}{\partial\rho}\right) + \hat{z}\left(\frac{V_\phi^{(m)}}{\rho} + \frac{\partial V_\phi^{(m)}}{\partial\rho} + i\frac{m}{\rho}V_\rho^{(m)}\right),$$

$$\nabla\mathbf{V}^{(m)} \equiv \begin{pmatrix} \frac{\partial V_\rho^{(m)}}{\partial\rho} & \frac{\partial V_\phi^{(m)}}{\partial\rho} & \frac{\partial V_z^{(m)}}{\partial\rho} \\ -im\frac{V_\rho^{(m)}}{\rho} - \frac{V_\phi^{(m)}}{\rho} & -im\frac{V_\phi^{(m)}}{\rho} + \frac{V_\rho^{(m)}}{\rho} & -im\frac{V_z^{(m)}}{\rho} \\ \frac{\partial V_\rho^{(m)}}{\partial z} & \frac{\partial V_\phi^{(m)}}{\partial z} & \frac{\partial V_z^{(m)}}{\partial z} \end{pmatrix}. \tag{A7}$$

The test functions are assumed to have a dependence of the form $e^{im\phi}$ so that the derivative with resect to ϕ gives a factor $+im$. It is possible then to reduce the initially three-dimensional problem into $2m_{max} + 1$ two-dimensional problems. For each m the system of equations to solve reads

$$2\pi \int (\nabla \times \mathbf{E}^{(m)}) \cdot (\nabla \times \tilde{\mathbf{E}}^{(m)}) - \left(k_0^2\mathbf{E}^{(m)} + \mu_0\omega^2\mathbf{P}^{(m)}\right) \cdot \tilde{\mathbf{E}}^{(m)}\rho\, d\rho\, dz = 0,$$

$$-2\pi \int \frac{e}{m}\left(\frac{\delta G}{\delta n}\right)_1^{(m)}(n_0\nabla \cdot \tilde{\mathbf{P}}^{(m)} + \nabla n_0 \cdot \tilde{\mathbf{P}}^{(m)}) + \frac{i\omega}{m}\sigma[n_0,\mathbf{P}^{(m)}] \cdot \nabla\mathbf{P}^{(m)}$$

$$-\left[(\omega^2 - i\gamma\omega)\mathbf{P}^{(m)} + \varepsilon_0\omega_p^2\left(\mathbf{E}^{(m)} + \mathbf{E}_{inc}^{(m)}\right)\right] \cdot \tilde{\mathbf{P}}^{(m)}\rho\, d\rho\, dz = 0, \tag{A8}$$

For the case of an incident plane wave propagating along the z axis, one has to solve the problem just for $m = \pm1$. Moreover by taking into account field parities, the solution for $m = 1$ can be related to the solution for $m = -1$, so that a single two-dimensional calculation becomes necessary [4,55]. For the dimer structure, on the other hand, the incident wave propagates perpendicularly to the z axis, so that the problem has to be solved for $m = 0 \ldots m_{max}$. Because, however, the system is deeply subwavelength only few terms ($m \leqslant 2$) give a non-negligible contribution.

Note that since the expression of the energy functional contains second-order derivatives, working variables associated to extra equations must be introduced so that the system only contains first-order derivatives [42].

[1] S. Raza, G. Toscano, A. P. Jauho, M. Wubs, and N. A. Mortensen, Unusual resonances in nanoplasmonic structures due to nonlocal response, Phys. Rev. B **84**, 121412 (2011).

[2] A. I. Fernández-Domínguez, P. Zhang, Y. Luo, S. A. Maier, F. J. García-Vidal, and J. B. Pendry, Transformation-optics insight into nonlocal effects in separated nanowires, Phys. Rev. B **86**, 241110(R) (2012).

[3] G. Toscano, S. Raza, A.-P. Jauho, N. A. Mortensen, and M. Wubs, Modified field enhancement and extinction by plasmonic nanowire dimers due to nonlocal response, Opt. Express **20**, 4176 (2012).

[4] C. Ciracì, Y. A. Urzhumov, and D. R. Smith, Effects of classical nonlocality on the optical response of three-dimensional plasmonic nanodimers, J. Opt. Soc. Am. B **30**, 2731 (2013).

[5] W. Yan and N. A. Mortensen, Nonclassical effects in plasmonics: An energy perspective to quantify nonclassical effects, Phys. Rev. B **93**, 115439 (2016).

[6] J. Zuloaga, E. Prodan, and P. Nordlander, Quantum description of the plasmon resonances of a nanoparticle dimer, Nano Lett. **9**, 887 (2009).

[7] W. Zhu, R. Esteban, A. G. Borisov, J. J. Baumberg, P. Nordlander, H. J. Lezec, J. Aizpurua, and K. B. Crozier, Quantum mechanical effects in plasmonic structures with subnanometre gaps, Nat. Commun. **7**, 11495 (2016).

[8] T. V. Teperik, P. Nordlander, J. Aizpurua, and A. G. Borisov, Robust Subnanometric Plasmon Ruler by Rescaling of the Nonlocal Optical Response, Phys. Rev. Lett. **110**, 263901 (2013).

[9] C. Ciracì, R. T. Hill, J. J. Mock, Y. A. Urzhumov, A. I. Fernandez-Dominguez, S. A. Maier, J. B. Pendry, A. Chilkoti, and D. R. Smith, Probing the ultimate limits of plasmonic enhancement, Science **337**, 1072 (2012).

[10] C. Ciracì, X. Chen, J. J. Mock, F. McGuire, X. Liu, S.-H. Oh, and D. R. Smith, Film-coupled nanoparticles by atomic layer

deposition: Comparison with organic spacing layers, Appl. Phys. Lett. **104**, 023109 (2014).

[11] S. Raza, S. Kadkhodazadeh, T. Christensen, M. Di Vece, M. Wubs, N. A. Mortensen, and N. Stenger, Multipole plasmons and their disappearance in few-nanometre silver nanoparticles, Nat. Commun. **6**, 8788 (2015).

[12] K. J. Savage, M. M. Hawkeye, R. Esteban, and A. G. Borisov, Revealing the quantum regime in tunneling plasmonics, Nature (London) **491**, 574 (2012).

[13] J. A. Scholl, A. García-Etxarri, A. L. Koh, and J. A. Dionne, Observation of quantum tunneling between two plasmonic nanoparticles, Nano Lett. **13**, 564 (2013).

[14] L. Lin, M. Zapata, M. Xiong, Z. Liu, S. Wang, H. Xu, A. G. Borisov, H. Gu, P. Nordlander, J. Aizpurua, and J. Ye, Nanooptics of plasmonic nanomatryoshkas: Shrinking the size of a core–shell junction to subnanometer, Nano Lett. **15**, 6419 (2015).

[15] G. Hajisalem, M. S. Nezami, and R. Gordon, Probing the quantum tunneling limit of plasmonic enhancement by third harmonic generation, Nano Lett. **14**, 6651 (2014).

[16] J. B. Lassiter, X. Chen, X. Liu, C. Ciracì, T. B. Hoang, S. Larouche, S.-H. Oh, M. H. Mikkelsen, and D. R. Smith, Third-harmonic generation enhancement by film-coupled plasmonic stripe resonators, ACS Photon. **1**, 1212 (2014).

[17] S. Kheifets, A. Simha, K. Melin, T. Li, and M. G. Raizen, Observation of Brownian motion in liquids at short times: Instantaneous velocity and memory loss, Science **343**, 1493 (2014).

[18] R. Chikkaraddy, B. de Nijs, F. Benz, S. J. Barrow, O. A. Scherman, E. Rosta, A. Demetriadou, P. Fox, O. Hess, and J. J. Baumberg, Single-molecule strong coupling at room temperature in plasmonic nanocavities, Nature (London) **535**, 127 (2016).

[19] W. Yan, M. Wubs, and N. A. Mortensen, Projected Dipole Model for Quantum Plasmonics, Phys. Rev. Lett. **115**, 137403 (2015).

[20] R. Esteban, A. G. Borisov, P. Nordlander, and J. Aizpurua, Bridging quantum and classical plasmonics with a quantum-corrected model, Nat. Commun. **3**, 825 (2012).

[21] A. Domps, P. G. Reinhard, and E. Suraud, Time-Dependent Thomas-Fermi Approach for Electron Dynamics in Metal Clusters, Phys. Rev. Lett. **80**, 5520 (1998).

[22] H. Xiang, X. Zhang, D. Neuhauser, and G. Lu, Size-dependent plasmonic resonances from large-scale quantum simulations, J. Phys. Chem. Lett. **5**, 1163 (2014).

[23] H. Xiang, M. Zhang, X. Zhang, and G. Lu, Understanding quantum plasmonics from time-dependent orbital-free density functional theory, J. Phys. Chem. C **120**, 14330 (2016).

[24] E. Madelung, Quantentheorie in hydrodynamischer form, Z. Phys. **40**, 322 (1927).

[25] F. Bloch, Bremsvermögen von atomen mit mehreren elektronen, Z. Phys. **81**, 363 (1933).

[26] D. Bohm and J. P. Vigier, Model of the causal interpretation of quantum theory in terms of a fluid with irregular fluctuations, Phys. Rev. **96**, 208 (1954).

[27] A. Eguiluz, S. Ying, and J. Quinn, Influence of the electron density profile on surface plasmons in a hydrodynamic model, Phys. Rev. B **11**, 2118 (1975).

[28] C. Schwartz and W. L. Schaich, Hydrodynamic models of surface plasmons, Phys. Rev. B **26**, 7008 (1982).

[29] E. Zaremba and H. C. Tso, Thomas–Fermi–Dirac–von Weizsäcker hydrodynamics in parabolic wells, Phys. Rev. B **49**, 8147 (1994).

[30] G. Manfredi, How to model quantum plasmas, arXiv:quant-ph/0505004.

[31] R. Ruppin, Plasmon frequencies of small metal spheres, J. Phys. Chem. Solids **39**, 233 (1978).

[32] A. Banerjee and M. K. Harbola, Hydrodynamical approach to collective oscillations in metal clusters, Phys. Lett. A **372**, 2881 (2008).

[33] J. E. Sipe, V. C. Y. So, M. Fukui, and G. I. Stegeman, Analysis of second-harmonic generation at metal surfaces, Phys. Rev. B **21**, 4389 (1980).

[34] A. Chizmeshya and E. Zaremba, Second-harmonic generation at metal surfaces using an extended Thomas–Fermi–von Weizsacker theory, Phys. Rev. B **37**, 2805 (1988).

[35] M. Scalora, M. A. Vincenti, D. de Ceglia, V. Roppo, M. Centini, N. Akozbek, and M. J. Bloemer, Second- and third-harmonic generation in metal-based structures, Phys. Rev. A **82**, 043828 (2010).

[36] C. Ciracì, E. Poutrina, M. Scalora, and D. R. Smith, Second-harmonic generation in metallic nanoparticles: Clarification of the role of the surface, Phys. Rev. B **86**, 115451 (2012).

[37] C. Ciracì, J. B. Pendry, and D. R. Smith, Hydrodynamic model for plasmonics: A macroscopic approach to a microscopic problem, ChemPhysChem **14**, 1109 (2013).

[38] S. Raza, S. I. Bozhevolnyi, M. Wubs, and N. A. Mortensen, Nonlocal optical response in metallic nanostructures, J. Phys.: Condens. Matter **27**, 183204 (2015).

[39] L. Stella, P. Zhang, F. J. García-Vidal, A. Rubio, and P. Garcia-Gonzalez, Performance of nonlocal optics when applied to plasmonic nanostructures, J. Phys. Chem. C **117**, 8941 (2013).

[40] G. Toscano, J. Straubel, A. Kwiatkowski, C. Rockstuhl, F. Evers, H. Xu, N. A. Mortensen, and M. Wubs, Resonance shifts and spill-out effects in self-consistent hydrodynamic nanoplasmonics, Nat. Commun. **6**, 7132 (2015).

[41] W. Yan, Hydrodynamic theory for quantum plasmonics: Linear-response dynamics of the inhomogeneous electron gas, Phys. Rev. B **91**, 115416 (2015).

[42] C. Ciracì and F. Della Sala, Quantum hydrodynamic theory for plasmonics: Impact of the electron density tail, Phys. Rev. B **93**, 205405 (2016).

[43] X. Li, H. Fang, X. Weng, L. Zhang, X. Dou, A. Yang, and X. Yuan, Electronic spill-out induced spectral broadening in quantum hydrodynamic nanoplasmonics, Opt. Express **23**, 29738 (2015).

[44] I. V. Tokatly, Time-dependent current density functional theory via time-dependent deformation functional theory: A constrained search formulation in the time domain, Phys. Chem. Chem. Phys. **11**, 4621 (2009).

[45] I. V. Tokatly, Quantum many-body dynamics in a Lagrangian frame: I. Equations of motion and conservation laws, Phys. Rev. B **71**, 165104 (2005).

[46] I. V. Tokatly, Quantum many-body dynamics in a Lagrangian frame: II. Geometric formulation of time-dependent density functional theory, Phys. Rev. B **71**, 165105 (2005).

[47] I. V. Tokatly, Time-dependent deformation functional theory, Phys. Rev. B **75**, 125105 (2007).

[48] J. Tao, X. Gao, G. Vignale, and I. V. Tokatly, Linear Continuum Mechanics for Quantum Many-Body Systems, Phys. Rev. Lett. **103**, 086401 (2009).

[49] X. Gao, J. Tao, G. Vignale, and I. V. Tokatly, Continuum mechanics for quantum many-body systems: Linear response regime, Phys. Rev. B **81**, 195106 (2010).

[50] T. Gould, G. Jansen, I. V. Tokatly, and J. F. Dobson, Quantum continuum mechanics made simple, J. Chem. Phys. **136**, 204115 (2012).

[51] G. Vignale and W. Kohn, Current-Dependent Exchange-Correlation Potential for Dynamical Linear Response Theory, Phys. Rev. Lett. **77**, 2037 (1996).

[52] J. C. Nickel, J. V. Parker, and R. W. Gould, Resonance Oscillations in a Hot Nonuniform Plasma Column, Phys. Rev. Lett. **11**, 183 (1963).

[53] I. Tokatly and O. Pankratov, Hydrodynamic theory of an electron gas, Phys. Rev. B **60**, 15550 (1999).

[54] I. V. Tokatly and O. Pankratov, Hydrodynamics beyond local equilibrium: Application to electron gas, Phys. Rev. B **62**, 2759 (2000).

[55] A. Eguiluz and J. Quinn, Hydrodynamic model for surface plasmons in metals and degenerate semiconductors, Phys. Rev. B **14**, 1347 (1976).

[56] D. Neuhauser, S. Pistinner, A. Coomar, X. Zhang, and G. Lu, Dynamic kinetic energy potential for orbital-free density functional theory, J. Chem. Phys. **134**, 144101 (2011).

[57] S. Laricchia, E. Fabiano, L. A. Constantin, and F. Della Sala, Generalized gradient approximations of the noninteracting kinetic energy from the semiclassical atom theory: Rationalization of the accuracy of the frozen density embedding theory for nonbonded interactions, J. Chem. Theory Comput. **7**, 2439 (2011).

[58] S. Laricchia, L. A. Constantin, E. Fabiano, and F. Della Sala, Laplacian-level kinetic energy approximations based on the fourth-order gradient expansion: Global assessment and application to the subsystem formulation of density functional theory, J. Chem. Theory Comput. **10**, 164 (2014).

[59] N. A. Mortensen, S. Raza, M. Wubs, T. Søndergaard, and S. I. Bozhevolnyi, A generalized non-local optical response theory for plasmonic nanostructures, Nat. Commun. **5**, 3809 (2014).

[60] J. P. Perdew and A. Zunger, Self-interaction correction to density-functional approximations for many-electron systems, Phys. Rev. B **23**, 5048 (1981).

[61] G. Vignale, C. A. Ullrich, and S. Conti, Time-Dependent Density Functional Theory Beyond the Adiabatic Local Density Approximation, Phys. Rev. Lett. **79**, 4878 (1997).

[62] E. K. U. Gross and W. Kohn, Local Density-Functional Theory of Frequency-Dependent Linear Response, Phys. Rev. Lett. **55**, 2850 (1985).

[63] N. Iwamoto and E. K. U. Gross, Correlation effects on the third-frequency-moment sum rule of electron liquids, Phys. Rev. B **35**, 3003 (1987).

[64] R. Nifosi, S. Conti, and M. P. Tosi, Dynamic exchange-correlation potentials for the electron gas in dimensionality $D=3$ and $D=2$, Phys. Rev. B **58**, 12758 (1998).

[65] Z. Qian and G. Vignale, Dynamical exchange-correlation potentials for an electron liquid, Phys. Rev. B **65**, 235121 (2002).

[66] S. Conti and G. Vignale, Elasticity of an electron liquid, Phys. Rev. B **60**, 7966 (1999).

[67] P. Hessler, J. Park, and K. Burke, Several Theorems in Time-Dependent Density Functional Theory, Phys. Rev. Lett. **82**, 378 (1999).

[68] R. D'Agosta and G. Vignale, Relaxation in Time-Dependent Current-Density-Functional Theory, Phys. Rev. Lett. **96**, 016405 (2006).

[69] C. A. Ullrich and G. Vignale, Collective intersubband transitions in quantum wells: A comparative density-functional study, Phys. Rev. B **58**, 15756 (1998).

[70] D. Yoo, N.-C. Nguyen, L. Martín Moreno, D. A. Mohr, S. Carretero-Palacios, J. Shaver, J. Peraire, T. W. Ebbesen, and S.-H. Oh, High-throughput fabrication of resonant meta-materials with ultrasmall coaxial apertures via atomic layer lithography, Nano Lett. **16**, 2040 (2016).

[71] X. Chen, N. C. Lindquist, D. J. Klemme, P. Nagpal, D. J. Norris, and S.-H. Oh, Split-wedge antennas with sub-5 nm gaps for plasmonic Nanofocusing, Nano Lett. **16**, 7849 (2016).

[72] COMSOL MULTIPHYSICS, http://www.comsol.com.

[73] C. Ciracì, Y. A. Urzhumov, and D. R. Smith, Far-field analysis of axially symmetric three-dimensional directional cloaks, Opt. Express **21**, 9397 (2013).

[74] U. Kreibig and M. Vollmer, *Optical Properties of Metal Clusters*, Springer Series in Materials Science Vol. 25 (Springer Science & Business Media, Berlin/Heidelberg, 2013).

[75] M. Barbry, P. Koval, F. Marchesin, R. Esteban, A. G. Borisov, J. Aizpurua, and D. Sánchez-Portal, Atomistic near-field nanoplasmonics: Reaching atomic-scale resolution in nanooptics, Nano Lett. **15**, 3410 (2015).